

1 ***Temperature impacts on fish physiology and resource abundance lead to faster growth but***
2 ***smaller fish sizes and yields under warming***

3

4 Max Lindmark^{a,1}, Asta Audzijonyte^b, Julia Blanchard^c, Anna Gårdmark^d

5 ^aSwedish University of Agricultural Sciences, Department of Aquatic Resources, Institute of
6 Coastal Research, Skolgatan 6, Öregrund 742 42, Sweden

7 ^bNature Research Centre, Akademijos 2, Vilnius, 20253, Lithuania

8 ^cInstitute for Marine and Antarctic Studies and Centre for Marine Socioecology, University of
9 Tasmania, 20 Castray Esplanade, Battery Point, Hobart, TAS 7000, Australia

10 ^dSwedish University of Agricultural Sciences, Department of Aquatic Resources, Box 7018,
11 750 07 Uppsala, Sweden

12

13 ¹Author to whom correspondence should be addressed. Current address:

14 Max Lindmark, Swedish University of Agricultural Sciences, Department of Aquatic
15 Resources, Institute of Marine Research, Turistgatan 5, 453 30 Lysekil, Sweden, Tel.:
16 +46(0)104784137, email: max.lindmark@slu.se

17

18

19

20

21

22

23 **Abstract**

24 Resolving the combined effect of climate warming and exploitation in a food web context is
25 key for predicting future biomass production, size-structure, and potential yields of marine
26 fishes. Previous studies based on mechanistic size-based food web models have found that
27 bottom-up processes are important drivers of size-structure and fisheries yield in changing
28 climates. However, we know less about the joint effects of ‘bottom-up’ and physiological
29 effects of temperature; how do temperature effects propagate from individual-level physiology
30 through food webs and alter the size-structure of exploited species in a community? Here we
31 assess how a species-resolved size-based food web is affected by warming through both these
32 pathways, and by exploitation. We parameterize a dynamic size spectrum food web model
33 inspired by the offshore Baltic Sea food web, and investigate how individual growth rates, size-
34 structure, relative abundances of species and yields are affected by warming. The magnitude
35 of warming is based on projections by the regional coupled model system RCA4-NEMO and
36 the RCP 8.5 emission scenario, and we evaluate different scenarios of temperature dependence
37 on fish physiology and resource productivity. When accounting for temperature-effects on
38 physiology in addition to on basal productivity, projected size-at-age in 2050 increases on
39 average for all fish species, mainly for young fish, compared to scenarios without warming. In
40 contrast, size-at-age decreases when temperature affects resource dynamics only, and the
41 decline is largest for young fish. Faster growth rates due to warming, however, do not always
42 translate to larger yields, as lower resource carrying capacities with increasing temperature tend
43 to result in declines in the abundance of larger fish and hence spawning stock biomass. These
44 results suggest that to understand how global warming affects the size structure of fish
45 communities, both direct metabolic effects and indirect effects of temperature via basal
46 resources must be accounted for.

47

48 **Key words**

49 Body size, climate change, fisheries yield, food web, metabolic theory, multi species, size

50 spectrum

51

52

53

54

55

56

57

58

59

60

61

62

63

64

65

66

67

68

69

70

71

72

73 **Introduction**

74 Climate change affects aquatic food webs directly by affecting species' distribution (Pinsky *et*
75 *al.* 2013), abundance (McCauley *et al.* 2015), body size (Daufresne *et al.* 2009; Baudron *et al.*
76 2014), and ecosystem function (Pontavice *et al.* 2019). Global retrospective analysis of
77 warming and fish population dynamics has revealed that the maximum sustainable yield of
78 scientifically assessed fish populations across ecoregions has already declined by 4.1% on
79 average between 1930 and 2010 due to climate change (Free *et al.* 2019). These results are also
80 matched in magnitude and direction by projections from an ensemble of mechanistic ecosystem
81 models, which predict ~5% decline in animal biomass for every 1 °C of warming, especially at
82 higher trophic levels (Lotze *et al.* 2019). Across a range of process-based ecosystem models,
83 declines in productivity of fish stocks and abundance of large fish have been linked to changes
84 in primary production or zooplankton abundance (Blanchard *et al.* 2012; Woodworth-Jefcoats
85 *et al.* 2013, 2015; Barange *et al.* 2014; Lotze *et al.* 2019; Heneghan *et al.* 2021; Tittensor *et al.*
86 2021). However, even in areas where warming is predicted to have positive effects on primary
87 production, fish productivity does not appear to increase (Free *et al.* 2019). This suggests that
88 fish population dynamics might be strongly influenced by other factors, such as temperature-
89 driven changes in recruitment, mortality or somatic growth (Free *et al.* 2019), yet the driving
90 mechanisms remain poorly understood.

91 Global warming is also predicted to cause reductions in the adult body size of organisms,
92 and this is often referred to as the third universal response to warming (Daufresne *et al.* 2009;
93 Sheridan & Bickford 2011; Forster *et al.* 2012). It is often attributed to the temperature-size
94 rule (TSR) is observed in a wide range of ectotherms (Forster *et al.* 2012). This is an
95 intraspecific rule stating that individuals reared at warmer temperatures develop faster, mature
96 earlier but reach smaller adult body sizes (Atkinson 1994; Ohlberger 2013). In line with TSR
97 expectations, faster growth rates or larger size-at-age of young life stages are commonly found

98 in both experimental, field data and modelling studies (Thresher *et al.* 2007; Neuheimer *et al.*
99 2011; Ohlberger *et al.* 2011; Neuheimer & Grønkjaer 2012; Baudron *et al.* 2014; Huss *et al.*
100 2019; van Dorst *et al.* 2019). Similarly, declines in maximum or asymptotic body size of fish
101 have been reported to correlate with warming trends for a number of commercially exploited
102 marine fishes (Baudron *et al.* 2014; van Rijn *et al.* 2017; Ikpewe *et al.* 2020). However, in
103 intensively fished stocks, observed adult body sizes can decrease also for other reasons,
104 including direct removals of large fish, or evolution towards earlier maturing and fast growth
105 in response to fishing (Jorgensen *et al.* 2007; Audzijonyte *et al.* 2013). Moreover, decreasing
106 adult fish size in warming waters is by far not universal. For example, no clear negative effects
107 of warming on the body size or growth of large fish could be found in a recent experimental
108 study (Barneche *et al.* 2019), or in a semi-controlled lake heating experiment (Huss *et al.* 2019).
109 Similarly, across 335 coastal fish species mean species body size was similarly likely to be
110 larger or smaller in warmer waters (Audzijonyte *et al.* 2020). Also Tu *et al.* (2018) found that
111 temperature had a relatively minor effect on fish size structure compared to fishing, when
112 assessing 28 stocks from the North Sea, US west coast and Eastern Bering Sea. Even when
113 combined with fishing, only 44% of variation in size structure could be explained. Thus, the
114 effects of temperature on body sizes may be more complex than often depicted, and we still do
115 not fully understand the mechanisms by which temperature affects growth and body size over
116 ontogeny (Ohlberger 2013; Audzijonyte *et al.* 2019). Increasing our understanding of these
117 mechanisms is important because body size is a key trait in aquatic ecosystems (Andersen *et*
118 *al.* 2016) and warming-induced changes in growth and size-at-age of fish populations could
119 have implications not only for biomass and productivity, but also ecosystem structure and
120 stability (Audzijonyte *et al.* 2013).

121 Physiologically structured models can address the complex interplay of direct and indirect
122 temperature impacts on food webs, as they account for the food and size dependence of body

123 growth through ecological interactions using bioenergetic principles. Recent applications have
124 demonstrated decreasing maximum body sizes in fish communities due to changes in plankton
125 abundance or size (Woodworth-Jefcoats *et al.* 2019). Similar body size responses emerge in
126 models that focus on temperature-dependence of physiological processes, such as metabolism
127 and feeding rates (Lefort *et al.* 2015; Guiet *et al.* 2016; Woodworth-Jefcoats *et al.* 2019), but
128 it remains unclear to what extent these community body size shifts are driven by declining
129 abundance of large fish versus changes in size-at-age across a range of ages.

130 To explore how direct and indirect effects of warming impact marine food web size structure
131 and fisheries yields, we evaluate the impacts of temperature-driven changes in resource
132 productivity and individual fish physiology using an example case of the Baltic Sea. The Baltic
133 Sea constitutes a great example system, as it is a relatively well understood and species poor
134 system (Mackenzie *et al.* 2007; Casini *et al.* 2009) that also is one of the warming hotspots
135 globally (Belkin 2009). By using a temperature-dependent size spectrum model we analyse a
136 set of different scenarios where either fish physiology, basal resources, or both depend on
137 temperature, and contrast these scenarios to one another and to non-warming scenarios. We
138 investigate the mechanisms of warming effects on body growth trajectories (size-at-age),
139 average body sizes, population size-structure and fisheries reference points.

140

141 **Materials and Methods**

142 In this section, we will describe the food web the model is parameterized to, the equations of
143 the multi-species size spectrum model, how temperature dependence is implemented in the
144 model, how the model is calibrated and lastly, how the effects of temperature are evaluated.

145

146 ***Food web***

147 We developed a multi-species size spectrum model (MSSM) (Scott *et al.* 2014), parameterized
148 to represent a simplified version of the food web in the offshore pelagic south-central Baltic
149 Sea ecosystem (Baltic proper) (ICES sub divisions 25-29+32, Fig. S2, *Supporting Information*)
150 and account for temperature-dependence of processes within and between individuals (Fig. 1).
151 This size structured food web is here characterized by three fish species: Atlantic cod (*Gadus*
152 *morhua*), sprat (*Sprattus sprattus*) and herring (*Clupea harengus*), and two background
153 resource spectra constituting food for small fish (pelagic and benthic resources). In the south-
154 central Baltic Sea, these fish species are dominant in terms of biomass, they are the most
155 important species commercially and they all have analytical stock assessments (ICES 2021).
156 The pelagic background resource spectrum represents mainly phyto- and zooplankton while
157 the benthic background resource spectrum represents benthic invertebrates, gobiidaes and
158 small flatfish.

159

160 ***Size spectrum model***

161 The model is based on source code for the multi-species implementation of size spectrum
162 models in the ‘R’-package *mizer* (v1.1) (Blanchard *et al.* 2014; Scott *et al.* 2014; R Core Team
163 2020), which has been extended to include multiple background resources
164 (<https://github.com/sizespectrum/mizerMR>) and temperature-scaling of key physiological
165 processes. In this section we describe the key elements of the MSSM using the same notation
166 when possible as in previous multispecies *mizer* models for consistency (Blanchard *et al.* 2014;
167 Scott *et al.* 2014, 2018).

168 In MSSMs, individuals are characterized by their weight (w) and species identity (i). The
169 core equation is the McKendrik-von Foerster equation. Here it describes the change in
170 abundance-at-size through time, $N_i(w)$, from food dependent somatic growth and mortality,
171 based on bioenergetic principles (explicit modelling of energy acquisition and use):

172
$$\frac{\partial N_i(w)}{\partial t} + \frac{\partial g_i(w)N_i(w)}{\partial w} = -\mu_i(w)N_i(w) \quad (1)$$

173 where $g_i(w)$ (g year^{-1}) is somatic growth (dependent on the availability of food) and $\mu_i(w)$
 174 (year^{-1}) is total mortality. At the boundary weight (w_0 , egg size), the influx of individuals is
 175 given by constant recruitment, which occurs at every model time step. Total mortality is the
 176 sum of the background-, starvation-, fishing-, and predation mortality. The constant species-
 177 specific allometric background mortality, $\mu_{bac,i}$, representing density- and predation
 178 independent sources of mortality, such as ageing, diseases, predation from species not included
 179 in the model, depends on the asymptotic weight of a species W_i^{n-1} and is given by:

180
$$\mu_{bac,i} = \mu_0 W_i^{n-1} \quad (2)$$

181 where n is the mass-exponent of maximum consumption rate (Hartvig *et al.* 2011) and μ_0 is an
 182 allometric constant. Starvation mortality ($\mu_{stv,i}$) is assumed to be proportional to energy
 183 deficiency (defined in Eq. 11) and inversely proportional to body mass (weight, w), and is
 184 defined as:

185
$$\mu_{stv,i}(w) = \begin{cases} 0 & \alpha f_i(w) h_i w^n > k_{met,i} w^p \\ \frac{k_{met,i} w^p - \alpha f_i(w) h_i w^n}{\xi w} & \text{otherwise} \end{cases} \quad (3)$$

186 where ξ , the fraction of energy reserves, is 0.1 (Hartvig *et al.* 2011). Instantaneous fishing
 187 mortality ($\mu_{fis,i}$) (year^{-1}) is defined as:

188
$$\mu_{fis,i}(w_i) = S_i(w) F_i \quad (4)$$

189 where S_i is the selectivity (for simplicity, we assumed knife-edge selectivity with weight at
 190 first catch corresponding to weight at maturation), and F_i is fishing mortality. Predation
 191 mortality ($\mu_{pre,j}$) for a prey species (or resource) j with weight w_j equals the amount consumed
 192 by predator species i with weight w_i :

193
$$\mu_{pre,j}(w_j) = \sum_i \int \phi_i \left(\frac{w_j}{w_i} \right) (1 - f_i(w_i)) \gamma_i w_i^q \theta_{i,j} N_i(w_i) dw \quad (5)$$

194 where $\theta_{i,j}$ is the non-size based preference of species i on species j , and ϕ_i describes the
 195 weight-based preference from the log-normal selection model (see below) (Ursin 1973).
 196 Satiation determines the feeding level $f_i(w)$ and is represented in the model with a Holling
 197 functional response type II. Satiation varies from 0 (no satiation) to 1 (full satiation):

$$198 \quad f_i(w) = \frac{E_{enc,i}(w)}{E_{enc,i}(w) + h_i w^n} \quad (6)$$

199 $h_i w^n$ is the allometric maximum consumption rate and $E_{enc,i}(w)$ is the encountered food (mass
 200 per time). The amount of encountered food for a predator of body weight w is given by the
 201 available food in the system multiplied with the search volume, $\gamma_i w^q$. Here, available food,
 202 $E_{ava,i}$, is the integral of the biomass of all prey species (j) and background resources (R) that
 203 falls within the prey preference ($\theta_{i,j}$, $\theta_{i,R}$) and size-selectivity (ϕ_i) of predator species i :

$$204 \quad E_{ava,i}(w) = \int \left(\sum_R \theta_{i,R} N_R(w_R) + \sum_j \theta_{i,j} N_j(w_j) \right) \phi_i \left(\frac{w_j}{w_i} \right) w_j dw_p \quad (7)$$

205 where w_j is the weight of prey, $\theta_{i,R}$ is the preference of species i for resource R , and j indicates
 206 prey (fish) species. Note that in contrast to other MSSMs (e.g., Blanchard *et al.* 2014) species
 207 in our model do not have specific preferences for other size-structured species (all values in
 208 the species interaction matrix $\theta_{i,R}$ are set to 1). However, they have different preferences for
 209 the two background resources. This helps to account for different feeding of sprat, herring and
 210 cod on benthic and pelagic resources. The size-selectivity of feeding, $\phi_i \left(\frac{w_j}{w_i} \right)$, is given by a
 211 log-normal selection function (Ursin 1967):

$$212 \quad \phi_i \left(\frac{w_j}{w_i} \right) = \exp \left[\frac{- \left(\ln \left(\frac{w_i}{(w_j \beta_i)} \right) \right)^2}{2 \sigma_i^2} \right] \quad (8)$$

213 where parameters β_i and σ_i are the preferred predator-prey mass ratio and the standard
214 deviation of the log-normal distribution, respectively. The amount of available prey of suitable
215 sizes (Eq. 7) is multiplied with the allometric function describing the search volume ($\gamma_i w^q$).
216 The allometric search volume coefficient is calculated as:

$$217 \quad \gamma_i(f_0) = \frac{f_0 h_i \beta_i^{2-\lambda} \exp\left(-\frac{(\lambda-2)^2 \sigma_i^2}{2}\right)}{(1-f_0)\sqrt{2\pi}\kappa\sigma_i} \quad (9)$$

218 (Andersen & Beyer 2006; Scott *et al.* 2018). The actual biomass of food encountered,
219 $E_{enc,i}(w)$, is defined as:

$$220 \quad E_{enc,i}(w) = \gamma_i w^q E_{ava,i}(w) \quad (10)$$

221 where q is the size-scaling exponent of the search volume. The rate at which food is consumed
222 is given by the product $f_i(w)h_i w^n$, which is assimilated with efficiency α and used to cover
223 metabolic costs. Metabolic costs scale allometrically as $k_{met,i} w^p$. The net energy, $E_{net,i}$, is
224 thus:

$$225 \quad E_{net,i}(w) = \max(0, \alpha f_i(w) h_i w^n - k_{met,i} w^p) \quad (11)$$

226 which is allocated to growth or reproduction. The allocation to reproduction (ψ_i) increases
227 smoothly from 0 around the weight maturation, $w_{mat,i}$, to 1 at the asymptotic weight, W_i ,
228 according to the function:

$$229 \quad \psi_i = \left[1 + \left(\frac{w}{w_{mat,i}} \right)^{-m} \right]^{-1} \left(\frac{w}{W_i} \right)^{1-n} \quad (12)$$

230 where m determines the steepness of the energy allocation curve, or how fast the allocation
231 switches from growth to reproduction at around the maturation size (Andersen 2019). This
232 function results in the growth rate, $g_i(w)$,

$$233 \quad g_i(w) = E_{net,i}(w)(1 - \psi_i(w)) \quad (13)$$

234 which approximates a von Bertalanffy growth curve when the feeding level is constant (Hartvig
235 *et al.* 2011; Andersen 2019). Reproduction is given by the total egg production in numbers,

236 which is the integral of the energy allocated to reproduction multiplied by a reproduction
237 efficiency factor ($\epsilon, erepro$) divided by the egg weight, w_0 , and the factor 2, assuming only
238 females reproduce:

$$239 R_{phy,i} = \frac{\epsilon}{2w_0} \int N_{i(w)} E_{net,i}(w) \psi_i(w) dw \quad (14)$$

240 This total egg production (or physiological recruitment, $R_{phy,i}$) results in recruits via a
241 Beverton-Holt stock recruit relationship, such that recruitment approaches a maximum
242 recruitment for a species i ($R_{max,i}$), as the egg production increases,

$$243 R_i = R_{max,i} \frac{R_{phy,i}}{R_{phy,i} + R_{max,i}} \quad (15)$$

244 where $R_{max,i}$ is treated as a free parameter and is estimated in the calibration process by
245 minimizing the residual sum of squares between spawning stock biomass from stock
246 assessments and the MSSM. The calibration also ensures that the species coexist in the model.

247 The temporal dynamics of the background resource (N_R) spectra (benthic and pelagic) are
248 defined as:

$$249 \frac{\partial N_R(w, t)}{\partial t} = r_o w^{p-1} [\kappa w^{-\lambda} - N_R(w, t)] - \mu_{p,R}(w) N_R(w, t) \quad (16)$$

250 where $r_o w^{p-1}$ is the population regeneration rate, $\kappa w^{-\lambda}$ is the carrying capacity of the
251 background resource and $\mu_{p,R}$ is predation mortality on resource spectrum R , and λ is defined
252 as $-2 - q + n$ (Andersen 2019).

253

254 ***Temperature dependence of fish physiology and resource dynamics***

255 To study the effects of warming on the modelled ecosystem, we introduce temperature impacts
256 on size-structured species physiological rates and background resource growth dynamics
257 following the metabolic theory of ecology (Gillooly *et al.* 2001; Brown *et al.* 2004).
258 Temperature affects the rate of metabolism (Clarke & Johnston 1999; Gillooly *et al.* 2001),

259 and thus also other biological rates such as feeding and mortality (Brown *et al.* 2004; Englund
260 *et al.* 2011; Rall *et al.* 2012; Thorson *et al.* 2017). We therefore scale rates of individual
261 metabolism ($k_{met,i}w^p$), maximum consumption (h_iw^n), search volume (γ_iw^q) and
262 background mortality ($\mu_0W_i^{n-1}$) with temperature. Metabolism and consumption are key terms
263 in the energy budget of fish (Eqns. 11-13). Thus, growth rate is not temperature-dependent
264 directly but its relationship to temperature emerges from the temperature-scaling of metabolism
265 and consumption. In *mizer*, metabolism represents all metabolic costs, i.e., standard, activity,
266 and digestion. Henceforth, we assume $k_{met,i}w^p$ scales as standard metabolic rate and refer to
267 it as metabolism or metabolic rate. For simplicity reasons and to reduce the number of
268 parameters and scenarios we assume that all rates scale with temperature exponentially
269 according the Arrhenius temperature correction factor:

$$270 \quad r(T) = e^{\frac{A_v(T-T_{ref})}{kTT_{ref}}} \quad (17)$$

271 where A_v is the activation energy (eV) for individual rate v , T is temperature (K), T_{ref} is the
272 reference temperature (here 283.15 K, the temperature where the Arrhenius correction factor
273 equals 1), and k is Boltzmann's constant in eV K⁻¹ ($= 8.617 \times 10^{-5}$ eV K⁻¹). We chose an
274 exponential temperature dependence as it provides a good statistical fit to data, is widely
275 adopted, and because we assume that the projected change in ocean temperature in the studied
276 time range does not lead to temperatures above physiological optima (e.g. (Righton *et al.* 2010)
277 as an example for cod), whereafter physiological rates might be expected to decline. While
278 temperature likely affects other physiological processes as well (such as cost of growth
279 (Barneche *et al.* 2019) or food conversion efficiency (Handeland *et al.* 2008)), we focus on the
280 temperature effects on metabolism, maximum consumption, search volume and mortality, as
281 their temperature dependencies are relatively well documented (Pauly 1980; Brown *et al.* 2004;
282 Dell *et al.* 2011; Englund *et al.* 2011; Thorson *et al.* 2017; Lindmark *et al.* 2022).

283 Temperature also affects plankton and benthos organisms, represented in our model through
284 background resources. In most size spectrum models to date, climate affects primary
285 production (and in some cases zooplankton), and this is modelled by forcing the background
286 spectra to observed abundance-at-size of plankton from either remotely sensed variables such
287 as chlorophyll-a, or from output (e.g., net primary production) from earth-system models
288 (Blanchard *et al.* 2012; Barange *et al.* 2014; Jennings & Collingridge 2015; Canales *et al.* 2016;
289 Galbraith *et al.* 2017; Reum *et al.* 2019; Woodworth-Jefcoats *et al.* 2019). These differences
290 have been highlighted as a key source of ecosystem model uncertainties observed in global
291 applications of size-structured models (Lotze *et al.* 2019; Heneghan *et al.* 2021). In order to
292 isolate the effects of temperature on resource and physiological processes, we apply the
293 temperature scaling to the terms of the background resource's semi-chemostat growth equation
294 (Eq. 16), i.e., their biomass regeneration rate and carrying capacity. We use the same Arrhenius
295 correction factor with activation energy A_r , where r refers to background resource parameter.
296 We assume that as temperature goes up, the carrying capacity (κw^λ) declines at the same rate
297 as population regeneration ($r_0 w^{p-1}$) rate increases (Savage *et al.* 2004; Gilbert *et al.* 2014), i.e.

298 κ scales with temperature in proportion to $e^{\frac{-A_r(T-T_{ref})}{kT T_{ref}}}$. This is based on the metabolic theory
299 of ecology (MTE), which predicts that if nutrient levels are constant, higher respiration rates
300 lead to lower biomasses at carrying capacity (Savage *et al.* 2004; Bernhardt *et al.* 2018). To
301 simplify the analyses, our implementation of temperature effects on the background spectrum
302 assumes that its size structure is not affected by the temperature (the slope of the spectrum does
303 not change)—only the overall level of background resources. As an example, using the average
304 activation energy for resource carrying capacity (see next paragraph), the elevation of our
305 background resource spectra (abundance at the geometric mean weight), declines with 8.7%
306 with a 1°C increase in temperature, which is line with a previous study (Heneghan *et al.* 2019).

307 Activation energies are estimated with uncertainty and they vary substantially between
308 processes, species, and taxonomic groups. To account for this uncertainty, here we
309 parameterized 200 projections of the food web model using randomly sampled activation
310 energies from normal distributions with rate-specific means and standard deviations. For
311 metabolism and maximum consumption, we acquired means and standard deviations of
312 posterior distributions provided in (Lindmark *et al.* 2022). For search volume we assumed that
313 it scales identically to maximum consumption, because both rates are related to feeding
314 processes. For background mortality we assumed identical scaling to metabolism, as longevity
315 is linked to life span and metabolic rate (Brown *et al.* 2004; McCoy & Gillooly 2008; Munch
316 & Salinas 2009). For background resource activation energies, we use the point estimate of the
317 activation energy (slope from a linear regression of natural log of growth rate as a function of
318 Arrhenius temperature ($1/kT$ [eV $^{-1}$])) from experimental data in Savage *et al.* (2004) as the
319 mean. These data consisted of protists, algae and zooplankton, and were extracted using the
320 software WebPlotDigitizer v. 4.1 (Rohatgi 2012). The standard deviation was approximated by
321 finding the value that resulted in 95% of the normal distribution being within the confidence
322 interval of the linear regression. For each of the 200 parameter combinations, each of the six
323 rate activation energy parameters was sampled independently from their respective distribution
324 and the model was projected to 2050. We then quantified the overall mean response and the
325 ranges of predictions resulting from 200 randomly parameterised simulations and visualized it
326 for the analysis of growth (size-at-age) and mean size.

327 We acknowledge that these scenarios are very simplified for evaluating changes in resource
328 productivity versus physiology with warming, and that they do not necessarily reflect the
329 predicted conditions in the Baltic Sea, nor all the potential pathways by which climate changes
330 affects the environmental conditions in the Baltic Sea. However, the simplicity allows us to
331 contrast effects of warming on basal food resources versus individual physiology of fish.

332

333 ***Model calibration***

334 Here we present a summary of the calibration approach—a more detailed description of the
335 step-by-step calibration protocol can be found in *Model calibration and validation, Supporting*
336 *Information*. The model was calibrated to average spawning stock biomasses (SSB_i) from stock
337 assessment data for cod, herring and sprat (ICES 2013, 2015) in 1992-2002, using average
338 fishing mortalities (F_i) in the same time frame. Ideally, the period for calibration should exhibit
339 relative stability, but such periods do not exist in the Baltic Sea, which is greatly influenced by
340 anthropogenic activities and has undergone dramatic structural changes over the last four
341 decades (Möllmann *et al.* 2009). We chose to calibrate our model to the time period of 1992-
342 2002 as in Jacobsen *et al.* (2017), which is a period after an ecological regime shift,
343 characterized by high fishing mortality on cod, low cod and herring abundance and high sprat
344 abundance (Gårdmark *et al.* 2015) (Fig. S4). The cut-off at 2002 also ensured that we did not
345 calibrate the model to the period starting from mid 2000's when the growth capacity, condition,
346 proportion of large fish in the population, and reproductive capacity of cod started to decline
347 rapidly (Svedäng & Hornborg 2014; Casini *et al.* 2016; Mion *et al.* 2018, 2021; Neuenfeldt *et*
348 *al.* 2020).

349 Model calibration was done by tuning the maximum recruitment parameter $R_{max,i}$ for the
350 three fish species while holding temperatures at T_{ref} . $R_{max,i}$ determines the maximum number
351 of offspring that can be produced by a population in a given time step and serves as a density
352 independent cap on reproduction. This parameter determines how species will respond to
353 exploitation and perturbations, and is one of the main parameters that is calibrated in multi-
354 species models (e.g., Blanchard *et al.* 2014; Jacobsen *et al.* 2017). We used the "L-BFGS-B"
355 algorithm (Byrd *et al.* 1995) in the 'R'-optimization function 'optim' to minimize the residual
356 sum of squares between the natural log of spawning stock biomass estimated in stock

357 assessment output (ICES 2013, 2015) and those emergent in the model for the years 1992-
358 2002. The optimization procedure resulted in close agreement between SSB from the model
359 and from stock assessments in the calibration time frame. Projections from 1992 and 2012 also
360 generally tracked the assessment SSBs (correlation coefficients of 0.65, 0.94 and 0.54 for cod,
361 herring and sprat, respectively). However, hindcasts (1974-2012) revealed no correlation
362 between assessment SSB and the model, while for herring and cod the general trends were
363 captured relatively well. The low ability to reconstruct historical biomasses is likely due to the
364 regime shift occurring between 1988-1993 (Möllmann et al. 2009). Growth curves emerging
365 from the model were in close agreement with von Bertalanffy curves fitted to length-at-age
366 data from trawl surveys (Fig. S6), after a stepwise manual increase of the constant in the
367 allometric maximum-consumption rate (h_i) (*Supporting Information*). The level of density
368 dependence imposed by the stock-recruitment function (see Eq. 14-15) was also evaluated by
369 assessing the ratio of the physiological recruitment, $R_{phy,i}$, to the recruitment R_i (Jacobsen *et*
370 *al.* 2017) (*Supporting Information*). These final values mean that stock recruitment is sensitive
371 to the stock biomass, but there is some density dependence limiting recruitment (i.e., not all
372 spawn produced become recruits). The fishing mortality leading to the highest long-term yield
373 (F_{MSY}) from the model (estimated for one species at the time while keeping each species at
374 their mean assessment F_{MSY}) were in agreement with the assessment F_{MSY} for sprat and herring.
375 For cod, F_{MSY} is lower in the size-spectrum model than in stock assessments.

376

377 ***Analysis of responses to warming***

378 We analyse the effects of warming on the size-structure food web in two different ways: by
379 projecting the food web to 2050 with time-varying sea surface trends, and by projecting the
380 model for 200 years with fixed temperatures above or below T_{ref} . The first set of simulations
381 aimed to assess possible fish population responses to the expected temperature changes, while

382 the second was aimed at exploring effects of temperature on fisheries yield and F_{MSY} at steady
383 state.

384 For the time-varying simulations, models were projected with historical annual fishing
385 mortalities (1974-2012) (ICES 2013, 2015) and sea surface temperature trends (1970-2050,
386 acquired from the regional coupled model system RCA4-NEMO under the RCP 8.5 scenario)
387 (Dieterich *et al.* 2019; Gröger *et al.* 2019). These relative temperature trends (relative to mean
388 in 1970-1999) are scaled by adding a constant so that the average temperature in the in the
389 calibration time period is T_{ref} (10°C). To ensure steady state was reached before time-varying
390 fishing mortality and temperature was introduced (1974 and 1970, respectively), we applied a
391 100-year burn-in period using the first fishing mortality and temperature value in the respective
392 time series (Fig. S12). For each species, we used the fishing mortality at maximum long-term
393 ('sustainable') yield, F_{MSY} in the years 2012-2050 (Fig. S12). These were derived from the size
394 spectrum model by finding the fishing mortalities resulting in highest yields at T_{ref} (Fig. S9).
395 We evaluated the effects of warming on weight-at-age, population mean weight and
396 abundance-at-weight for each species. This was done for both absolute values, and by
397 comparing warming food webs in 2050 to a baseline scenario where no warming occurred post
398 1997 (the mid-point of calibration time window, where temperature averages T_{ref}) (Fig. S12).
399 In this way the three scenarios considered contrast the effects of temperature affecting fish
400 physiology, their resources or both.

401 For the non-time varying temperature projections we specified a range of constant (not time-
402 varying) temperatures and fishing mortalities, expressed as proportions of T_{ref} and F_{MSY} at the
403 reference temperature ($F_{MSY,T_{ref}}$), respectively, and projected the models to steady state (200
404 years). We explored scenarios where temperature ranged between 0.75 to 1.25 of T_{ref} , and F_{MSY}
405 ranged between 0.1 and 2 of $F_{MSY,T_{ref}}$. With the full factorial combination of these scenarios,

406 this gave a total of 1989 scenarios. These simulations were done to explore the effect of
407 temperature on fisheries yield and F_{MSY} .

408

409 **Results**

410 ***Effects of warming on size-at-age depend on physiological temperature-dependence***

411 The inclusion of temperature effects on fish physiological processes has a strong influence on
412 the projected size-at-age in 2050 under the RCP 8.5 emission scenario, relative to the baseline
413 projection (no warming) (Fig. 2). Temperature-dependence of feeding rates have a particularly
414 large effect (Fig. S15). Warming positively affects size-at-age when temperature affected
415 metabolism, maximum consumption, search volume and mortality, regardless of whether
416 temperature impacted background resource dynamics (Fig. 2). In contrast, the scenarios
417 without temperature-dependent physiological processes all lead to size-at-age decreasing with
418 warming (Fig. 2). In scenarios with temperature-dependent physiological processes, the effects
419 on size-at-age are positive and declines with age. When only resources are affected by
420 temperature, small individuals have the largest relative decrease in size-at-age, and this
421 negative effect of warming declines with age (Fig. 2).

422 Despite the relatively narrow range of activation energies for physiological rates considered
423 here (Fig. S3; Table S3), the uncertainty in projected size-at-age associated with variation in
424 the activation energies is large (Fig. 2). In the scenario where both physiology and resources
425 are affected by temperature, the range of predicted changes in size-at-age vary at approximately
426 +10% to +40% (Fig. 2). These changes in size-at-age seem to be driven by the temperature-
427 dependence of maximum consumption rate ($h_i w^n(T)$) increasing the actual consumption rates
428 ($f_i(w)h_i w^n(T)$), but having almost no effect on the feeding or satiation levels (Eq. 6; Fig.
429 S13).

430

431 ***Fewer large individuals cause reductions in mean population body size***

432 Increases in size-at-age (Fig. 2) do not always lead to increased mean body size in the
433 populations (Fig. 3), due to changes in the relative abundances at size and in this way shifting
434 population size structure (Fig. 4). Changes in the size-structure varied across species without a
435 clear and consistent pattern across species and scenarios.

436 The only scenario where mean body weight on average increases is where temperature only
437 affects physiology and not the resource (Fig. 3). In such cases, body weight increases with
438 warming, but only for cod and sprat. For cod this increase is strong and is driven by both faster
439 growth rates (larger size-at-age) and large increases in the abundance of large fish (~10 kg)
440 (Figs. 2, 4). For sprat the mean body weight in the populations increased only marginally and
441 is mostly driven by faster growth rates and increased relative abundance of fish above 10 g
442 (Figs. 2, 4). In contrast, scenarios where only resources are affected by temperature, relative
443 numbers of large individuals and therefore mean body size of all species goes down. For
444 herring, all scenarios lead to smaller mean body sizes in the population, and the relative (to
445 non-warming simulation) abundance-at-weight declines with mass in most of the size range,
446 with increases only in the very smallest size classes (< 1g; Fig. 4).

447

448 ***Temperature and fishing: higher sustained exploitation rates but reduced yields in warmer
449 environments***

450 Our simulations applying a range of stable (not time-varying) temperature and fishing scenarios
451 showed that warming led to higher or equal F_{MSY} (i.e., the fishing mortality leading to
452 maximum sustainable yield), but lower yields (Fig. 5-6). F_{MSY} declines with warming for
453 herring when only resources are temperature dependent, and F_{MSY} for sprat declines resources
454 are temperature dependent, else F_{MSY} increases. Yields however, decline for all species in all
455 scenarios except for cod when only physiological processes are temperature dependent. The

456 increase in F_{MSY} is likely due to the enhanced growth rates, which allow higher fishing
457 mortalities without impairing population growth. Cod in the scenario with only physiological
458 scaling is the exemption. The model projects higher yields as temperature increase, due to the
459 increase in growth rate, average size and relative abundance of large individuals (See Figs. 2-
460 4). In general, the highest relative yield is found at the coolest temperatures and F slightly
461 lower than F_{MSY} at the reference temperature (Fig. 6). The decline in relative yields of herring
462 and sprat in all scenarios (Fig. 5) is likely driven by the warming-induced decline in abundance,
463 due to resource limitation (Fig. 4).

464

465 **Discussion**

466 ***Combined temperature impacts on fish growth rates, body size and fisheries yield***

467 Using a size-structured and species-resolved food web model, we demonstrate how climate
468 warming affects growth rates (size-at-age), population mean size and size-structure of
469 interacting exploited fish species and assess its implications for fisheries yield. To do so, we
470 contrasted the effects of warming on resource productivity and individual level physiology
471 (metabolism, feeding and background mortality) of fish. We found that warming leads to
472 increased size-at-age of fishes when temperature-dependence is included in physiological rates.
473 This effect is strongest in juveniles of all three fish species. Though, despite increased growth
474 rates, in most cases, warming leads to smaller mean body size in the population, lower
475 spawning stock biomass (biomass of mature fish) and reduced yields. When temperature affects
476 only the background resource species, the size-at-age declines for fish of all sizes.

477 Mechanistic that models explore warming-driven declines in community-wide average body
478 size often find these declines to be driven by lower food abundance or decreased energy transfer
479 efficiency in the food web, due to a combination of declines in plankton density and shifts
480 towards dominance of smaller plankton at higher temperatures (Lefort *et al.* 2015; Woodworth-

481 Jefcoats *et al.* 2015, 2019). This leads to a community wide decline in mean size of fish, where
482 large bodied species become relatively fewer. The cause of these community-level changes are
483 different from those expected at an individual species level, where temperature can either lead
484 to size-at-age changes over ontogeny (in accordance with the temperature-size rule), or a
485 change in the relative abundance of small vs large individuals. TSR (the temperature-size rule)
486 predicts higher growth rates and thus size-at-age of juveniles, but smaller adults body sizes
487 (Atkinson 1994), although the physiological processes that lead to these changes remain
488 debated (Audzijonyte *et al.* 2019). In our model, we include scenarios that reflect both warmer
489 temperatures impact on food abundance as well physiological changes in metabolism and food
490 intake rates. Scenarios with only temperature dependence of resource dynamics lead to declines
491 in size-at-age (that in addition were strongest in young fish). This does not match general
492 observations and predictions of how body growth is affected by warming (Thresher *et al.* 2007;
493 Morita *et al.* 2010; Huss *et al.* 2019; Lindmark *et al.* 2022), and is not in accordance with the
494 TSR. In contrast, inclusion of physiological temperature dependence leads to projections more
495 in line with general observations from field data, which often find increased size-at-age that is
496 strongest and positive for small individuals, and that this effect diminishes over ontogeny
497 (Thresher *et al.* 2007; Huss *et al.* 2019).

498 The increase in body growth that we find is in general not sufficient for maintaining
499 similar mean population body sizes and size-structure, if resource carrying capacities decline
500 with warming, because this reduces the relative abundance of large fish. Mean body size in the
501 population and yields therefore decline in the scenario with temperature dependence of both
502 resource dynamics and physiology. These predictions on the net effect of warming are in line
503 with similar models using empirically derived static plankton spectra (Blanchard *et al.* 2012;
504 Canales *et al.* 2016; Woodworth-Jefcoats *et al.* 2019), and empirical studies (van Dorst *et al.*
505 2019). If, however, resource carrying capacity would not decline with temperature, our results

506 show that the increased body growth potential in fish due to higher metabolic and feeding rates
507 can lead to changes towards dominance of larger fish in some populations. This is important to
508 consider, given that predictions about effects of climate change on primary production are
509 uncertain and show large regional variability (Steinacher *et al.* 2010). These results show that
510 it is important to account for both direct (physiology) and indirect (resources) effects of
511 temperature in order to explain results such as increased growth rates and size-at-age but
512 overall smaller-bodied populations, as also found in other studies (Ohlberger *et al.* 2011;
513 Ohlberger 2013; Neubauer & Andersen 2019; Gårdmark & Huss 2020).

514 In fisheries stock assessment, plastic body growth was generally thought to be less important
515 for stock dynamics than environmentally driven recruitment variation, density dependence at
516 early life stages and mortality (Hilborn & Walters 1992; Lorenzen 2016). Due to the
517 accumulating evidence of time-varying and climate-driven changes in vital rates (survival,
518 growth and reproduction), their relative importance for fisheries reference points and targets
519 are now becoming acknowledged (Thorson *et al.* 2015; Lorenzen 2016). In our modelling
520 system, we find that maximum sustainable yields (MSY) and the fishing mortality leading to
521 MSY , i.e., F_{MSY} , vary with both temperature and between modelling scenarios, and largely
522 depends on the net effect of temperature on abundance-at-size and body growth rates. When
523 temperature affects both the background resources (mainly declining carrying capacity) and
524 fish physiology, warming tends to increase F_{MSY} , but the yield (MSY) derived at this
525 exploitation rate is lower. The decline in yields with warming is due to reduced resource
526 availability, lowering overall fish abundance, and is in line with earlier studies (Blanchard *et*
527 *al.* 2012; Lotze *et al.* 2019). In addition, the warming-induced decline in relative abundance of
528 fish above minimum size caught in fisheries further decreases yields in our model. At the same
529 time, higher growth rates (size-at-age), occurring when temperature affects metabolism and
530 intake rates in particular, can cause F_{MSY} to increase with warming (Thorson *et al.* 2015). These

531 reference levels should not be viewed as absolute reference points, and the specific results may
532 depend on the model calibration procedure. However, our findings suggest that climate change
533 predictions on fisheries productivity must consider both temperature impacts on vital rates, in
534 particular body growth, as well as bottom-up processes and their effects on both the overall
535 abundance and size-structure of the stock. It also indicates that because productivity may
536 decline with warming in large parts of the oceans (Kwiatkowski *et al.* 2020) (although there is
537 large variation in these predictions across ecosystems (Steinacher *et al.* 2010)), reduced
538 fisheries yields may be common in a warming world.

539

540 ***Parameterizing and modelling temperature effects***

541 Including physiological temperature-dependence can strongly influence predictions of
542 warming-effects and it allows for detailed understanding of temperature effects on populations
543 and food webs via both individual bioenergetics and the emerging responses in fish body
544 growth rates. However, it also requires more parameters, which in turn may vary across species.
545 This could reduce generality of predictions and increased challenges in parameterizing models
546 of data poor systems. We approached this by applying random parameterization, rather than
547 fixed values of temperature dependence. To capture the uncertainty of our approach, we
548 sampled parameters from distributions based on estimates of activation energies of
549 physiological rates in the literature (Lindmark *et al.* 2022). This approach revealed that in terms
550 of body growth and mean body size in populations, the combination of activation energies can
551 determine whether the mean size increases or decreases with warming, and at what age body
552 sizes decline relative to the current temperatures (degree of decline in size-at-age). Hence,
553 better knowledge of the temperature-dependence of rates of biological processes is needed and
554 these parameters should be chosen carefully, and their uncertainty acknowledged in future
555 modelling studies.

556 To disentangle temperature effects on background resources and physiological processes,
557 we modelled temperature dependence of resources by scaling their parameters with the same
558 general Arrhenius equation (Gillooly *et al.* 2001) that we used to scale the physiological
559 processes in fish. Other similar studies that use size spectrum models with physiological
560 temperature-dependence instead import the plankton spectra from climate and earth systems
561 models (Woodworth-Jefcoats *et al.* 2019) or from satellite data (Canales *et al.* 2016). Such
562 approaches may lead to predictions that are more relevant for a specific system. However, it
563 also becomes more difficult to separate the mechanisms behind the observed changes, as the
564 resource dynamics then are externally forced and cannot respond to changes in the modelled
565 food web. Moreover, populating a resource size spectrum based on observed data can be
566 difficult as observed spectra result from both predation and bottom-up processes. As an
567 alternative, our approach of directly scaling the carrying capacity or turnover rates of
568 background resources with temperature provides a coherent way to model temperature-
569 dependencies across trophic levels. The resource dynamics are then impacted by any warming-
570 driven changes in predators, as well as inherent temperature-dependent dynamics, rather than
571 driven by external data (Canales *et al.* 2016) or models (e.g., Woodworth-Jefcoats *et al.* 2019).
572 On the downside, this approach means relying on many major simplifications with respect to
573 resource dynamics. In addition, our scenarios only include identical temperature dependencies
574 and baseline carrying capacity of pelagic and benthic resources, and only negative effects of
575 temperature on resource carrying capacity. These may reflect the global decline in primary
576 production (Steinacher *et al.* 2010) commonly predicted by coupled climate models. It would
577 be straightforward to model increases in carrying capacity with our approach by using positive
578 activation energies. It is also possible to include temperature-effects of the slope of the size
579 spectrum, as this is often found to be negatively related to temperature (e.g., (Morán *et al.* 2010;

580 Yvon-Durocher *et al.* 2011; Canales *et al.* 2016; Woodworth-Jefcoats *et al.* 2019), but see also
581 Barnes *et al.* (2011) for a non-significant negative effect on the size-spectrum slope).

582

583 **Conclusion**

584 Ecological forecasting is inherently difficult, and climate change alters the already complex
585 causal pathways that drive ecosystem dynamics. Size spectrum models have successfully been
586 used to evaluate size-based mechanisms and structuring forces in ecosystems (Andersen &
587 Pedersen 2009; Szwalski *et al.* 2017; Reum *et al.* 2019). In this study, we have highlighted
588 the important role of temperature-dependent individual-level metabolism and feeding rates for
589 emerging size-at-age patterns that are in line with general observations and predictions (e.g.,
590 with the TSR). These also affect the levels of exploitation that leads to maximum sustainable
591 yields, and the corresponding yields. Hence, accounting for temperature-dependence of both
592 ecological and physiological processes underlying population dynamics is important for
593 increasing our understanding of how and by which processes climate change affects individuals
594 in food webs and resulting effects on fisheries yields, which is needed to generalize across
595 systems and into novel conditions.

596

597 **Acknowledgements**

598 Thanks to Romain Forestier and Jonatan Reum for contributing to developing code on
599 temperature-dependence in *mizer* during a workshop, Ken Haste Andersen for helpful
600 discussion on model calibration, Christian Dietrich for providing temperature data. We also
601 thank two anonymous reviewers for feedback that improved the manuscript, ICES staff and all
602 involved in all stages of data collections, the helpful *mizer* community, Elizabeth Duskey and
603 Magnus Huss for providing useful input. This study was supported by grants from the Swedish

604 Research Council FORMAS (no. 217-2013-1315) and the Swedish Research Council (no.
605 2015-03752) (both to AG).

606

607 **Author contributions**

608 The code was first developed from *mizer* (Scott *et al.* 2019) by AA to include multiple
609 background resources, all authors contributed to developing the code to include temperature.
610 ML conceived the idea. All authors contributed to study design. ML parameterized the model
611 with input from AG. ML performed analysis and wrote the first draft. All authors contributed
612 to writing the paper and to revisions.

613

614 **Data availability**

615 All model code (parameterization, calibration and analysis) and data are available on GitHub
616 (<https://github.com/maxlindmark/mizer-rewiring/tree/rewire-temp/baltic>) and will be
617 deposited on Zenodo upon publication.

618

619 **References**

620 Andersen, K.H. (2019). *Fish Ecology, Evolution, and Exploitation: A New Theoretical
621 Synthesis*. Princeton University Press.

622 Andersen, K.H., Berge, T., Gonçalves, R.J., Hartvig, M., Heuschele, J., Hylander, S., *et al.*
623 (2016). Characteristic Sizes of Life in the Oceans, from Bacteria to Whales. *Ann Rev
624 Mar Sci*, 8, 217–241.

625 Andersen, K.H. & Beyer, J.E. (2006). Asymptotic Size Determines Species Abundance in the
626 Marine Size Spectrum. *The American Naturalist*, 168, 8.

627 Andersen, K.H. & Pedersen, M. (2009). Damped trophic cascades driven by fishing in
628 model marine ecosystems. *Proceedings of the Royal Society of London B: Biological
629 Sciences*, 277, 795–802.

630 Atkinson, D. (1994). Temperature and organism size—A biological law for ectotherms? In:
631 *Advances in Ecological Research*. Elsevier, pp. 1–58.

632 Audzijonyte, A., Barneche, D.R., Baudron, A.R., Belmaker, J., Clark, T.D., Marshall, C.T., *et
633 al.* (2019). Is oxygen limitation in warming waters a valid mechanism to explain
634 decreased body sizes in aquatic ectotherms? *Global Ecology and Biogeography*, 28,
635 64–77.

636 Audzijonyte, A., Kuparinen, A., Gorton, R. & Fulton, E.A. (2013). Ecological consequences
637 of body size decline in harvested fish species: positive feedback loops in trophic
638 interactions amplify human impact. *Biology Letters*, 9, 20121103.

639 Audzijonyte, A., Richards, S.A., Stuart-Smith, R.D., Pecl, G., Edgar, G.J., Barrett, N.S., *et al.*
640 (2020). Fish body sizes change with temperature but not all species shrink with
641 warming. *Nat Ecol Evol*, 4, 809–814.

642 Barange, M., Merino, G., Blanchard, J.L., Scholtens, J., Harle, J., Allison, E.H., *et al.* (2014).
643 Impacts of climate change on marine ecosystem production in societies dependent on
644 fisheries. *Nature Clim Change*, 4, 211–216.

645 Barneche, D.R., Jahn, M. & Seebacher, F. (2019). Warming increases the cost of growth in a
646 model vertebrate. *Functional Ecology*, 33, 1256–1266.

647 Barnes, C., Irigoien, X., De Oliveira, J.A.A., Maxwell, D. & Jennings, S. (2011). Predicting
648 marine phytoplankton community size structure from empirical relationships with
649 remotely sensed variables. *J Plankton Res*, 33, 13–24.

650 Baudron, A.R., Needle, C.L., Rijnsdorp, A.D. & Marshall, C.T. (2014). Warming
651 temperatures and smaller body sizes: synchronous changes in growth of North Sea
652 fishes. *Global Change Biology*, 20, 1023–1031.

653 Belkin, I.M. (2009). Rapid warming of large marine ecosystems. *Progress in Oceanography*,
654 81, 207–213.

655 Bernhardt, J.R., Sunday, J.M. & O'Connor, M.I. (2018). Metabolic Theory and the
656 Temperature-Size Rule Explain the Temperature Dependence of Population Carrying
657 Capacity. *The American Naturalist*, 192, 687–697.

658 Blanchard, J.L., Andersen, K.H., Scott, F., Hintzen, N.T., Piet, G. & Jennings, S. (2014).
659 Evaluating targets and trade-offs among fisheries and conservation objectives using a
660 multispecies size spectrum model. *Journal of Applied Ecology*, 51, 612–622.

661 Blanchard, J.L., Jennings, S., Holmes, R., Harle, J., Merino, G., Allen, J.I., *et al.* (2012).
662 Potential consequences of climate change for primary production and fish production
663 in large marine ecosystems. *Philosophical Transactions of the Royal Society of
664 London, Series B: Biological Sciences*, 367, 2979–2989.

665 Brown, J.H., Gillooly, J.F., Allen, A.P., Savage, V.M. & West, G.B. (2004). Toward a
666 metabolic theory of ecology. *Ecology*, 85, 1771–1789.

667 Byrd, R.H., Lu, Peihuang., Nocedal, Jorge. & Zhu, Ciyou. (1995). A Limited Memory
668 Algorithm for Bound Constrained Optimization. *SIAM J. Sci. Comput.*, 16, 1190–
669 1208.

670 Canales, T.M., Law, R. & Blanchard, J.L. (2016). Shifts in plankton size spectra modulate
671 growth and coexistence of anchovy and sardine in upwelling systems. *Canadian
672 Journal of Fisheries and Aquatic Sciences*, 73, 611–621.

673 Casini, M., Hjelm, J., Molinero, J.-C., Lövgren, J., Cardinale, M., Bartolino, V., *et al.* (2009).
674 Trophic cascades promote threshold-like shifts in pelagic marine ecosystems.
675 *Proceedings of the National Academy of Sciences, USA*, 106, 197–202.

676 Casini, M., Käll, F., Hansson, M., Plikshs, M., Baranova, T., Karlsson, O., *et al.* (2016).
677 Hypoxic areas, density-dependence and food limitation drive the body condition of a
678 heavily exploited marine fish predator. *Royal Society Open Science*, 3, 160416.

679 Clarke, A. & Johnston, N.M. (1999). Scaling of metabolic rate with body mass and
680 temperature in teleost fish. *Journal of Animal Ecology*, 68, 893–905.

681 Daufresne, M., Lengfellner, K. & Sommer, U. (2009). Global warming benefits the small in
682 aquatic ecosystems. *Proceedings of the National Academy of Sciences, USA*, 106,
683 12788–12793.

684 Dell, A.I., Pawar, S. & Savage, V.M. (2011). Systematic variation in the temperature
685 dependence of physiological and ecological traits. *Proceedings of the National
686 Academy of Sciences*, 108, 10591–10596.

687 Dieterich, C., Wang, S., Schimanke, S., Gröger, M., Klein, B., Hordoir, R., *et al.* (2019).
688 Surface Heat Budget over the North Sea in Climate Change Simulations. *Atmosphere*,
689 10, 272.

690 van Dorst, R.M., Gårdmark, A., Svanbäck, R., Beier, U., Weyhenmeyer, G.A. & Huss, M.
691 (2019). Warmer and browner waters decrease fish biomass production. *Global
692 Change Biology*, 25, 1395–1408.

693 Englund, G., Öhlund, G., Hein, C.L. & Diehl, S. (2011). Temperature dependence of the
694 functional response. *Ecology Letters*, 14, 914–921.

695 Forster, J., Hirst, A.G. & Atkinson, D. (2012). Warming-induced reductions in body size are
696 greater in aquatic than terrestrial species. *PNAS*, 109, 19310–19314.

697 Free, C.M., Thorson, J.T., Pinsky, M.L., Oken, K.L., Wiedenmann, J. & Jensen, O.P. (2019).
698 Impacts of historical warming on marine fisheries production. *Science*, 363, 979–983.

699 Galbraith, E.D., Carozza, D.A. & Bianchi, D. (2017). A coupled human-Earth model
700 perspective on long-term trends in the global marine fishery. *Nat Commun*, 8, 14884.

701 Gårdmark, A., Casini, M., Huss, M., van Leeuwen, A., Hjelm, J., Persson, L., *et al.* (2015).
702 Regime shifts in exploited marine food webs: detecting mechanisms underlying
703 alternative stable states using size-structured community dynamics theory. *Phil.
704 Trans. R. Soc. B*, 370, 20130262.

705 Gårdmark, A. & Huss, M. (2020). Individual variation and interactions explain food web
706 responses to global warming. *Philosophical Transactions of the Royal Society B:
707 Biological Sciences*, 375, 20190449.

708 Gilbert, B., Tunney, T.D., McCann, K.S., DeLong, J.P., Vasseur, D.A., Savage, V.M., *et al.*
709 (2014). A bioenergetic framework for the temperature dependence of trophic
710 interactions. *Ecology Letters*, 17, 902–914.

711 Gillooly, J.F., Brown, J.H., West, G.B., Savage, V.M. & Charnov, E.L. (2001). Effects of
712 size and temperature on metabolic rate. *Science*, 2248-2251.

713 Gröger, M., Arneborg, L., Dieterich, C., Höglund, A. & Meier, H.E.M. (2019). Summer
714 hydrographic changes in the Baltic Sea, Kattegat and Skagerrak projected in an
715 ensemble of climate scenarios downscaled with a coupled regional ocean–sea ice–
716 atmosphere model. *Clim Dyn*, 53, 5945–5966.

717 Guiet, J., Aumont, O., Poggiale, J.-C. & Maury, O. (2016). Effects of lower trophic level
718 biomass and water temperature on fish communities: A modelling study. *Progress in
719 Oceanography*, 146, 22–37.

720 Handeland, S.O., Imsland, A.K. & Stefansson, S.O. (2008). The effect of temperature and
721 fish size on growth, feed intake, food conversion efficiency and stomach evacuation
722 rate of Atlantic salmon post-smolts. *Aquaculture*, 283, 36–42.

723 Hartvig, M., Andersen, K.H. & Beyer, J.E. (2011). Food web framework for size-structured
724 populations. *Journal of Theoretical Biology*, 272, 113–122.

725 Heneghan, R.F., Galbraith, E., Blanchard, J.L., Harrison, C., Barrier, N., Bulman, C., *et al.*
726 (2021). Disentangling diverse responses to climate change among global marine
727 ecosystem models. *Progress in Oceanography*, 198, 102659.

728 Heneghan, R.F., Hatton, I.A. & Galbraith, E.D. (2019). Climate change impacts on marine
729 ecosystems through the lens of the size spectrum. *Emerging Topics in Life Sciences*,
730 3, 233–243.

731 Hilborn, R. & Walters, C.J. (1992). *Quantitative Fisheries Stock Assessment: Choice,
732 Dynamics and Uncertainty*. Springer, Norwell MA, USA.

733 Huss, M., Lindmark, M., Jacobson, P., van Dorst, R.M. & Gårdmark, A. (2019).
734 Experimental evidence of gradual size-dependent shifts in body size and growth of
735 fish in response to warming. *Glob Change Biol*, 25, 2285–2295.

736 ICES. (2013). *Report of the Baltic Fisheries Assessment Working Group (WGBFAS)* (No.
737 ICES CM 2013/ACOM:10.). 10-17 April 2013 ICES Headquarters, Copenhagen.

738 ICES. (2015). *Report of the Baltic Fisheries Assessment Working Group (WGBFAS)* (No.
739 ICES CM 2015/ACOM:10). 14-21 April 2015 ICES Headquarters, Copenhagen.

740 ICES. (2021). *Report of the Baltic Fisheries Assessment Working Group (WGBFAS)* (No.
741 3:53).

742 Ikpewe, I.E., Baudron, A.R., Ponchon, A. & Fernandes, P.G. (2020). Bigger juveniles and
743 smaller adults: Changes in fish size correlate with warming seas. *Journal of Applied
744 Ecology*, 58, 847–856.

745 Jacobsen, N.S., Burgess, M.G. & Andersen, K.H. (2017). Efficiency of fisheries is increasing
746 at the ecosystem level. *Fish and Fisheries*, 18, 199–211.

747 Jennings, S. & Collingridge, K. (2015). Predicting Consumer Biomass, Size-Structure,
748 Production, Catch Potential, Responses to Fishing and Associated Uncertainties in the
749 World's Marine Ecosystems. *PLOS ONE*, 10, e0133794.

750 Jorgensen, C., Enberg, K., Dunlop, E.S., Arlinghaus, R., Boukal, D.S., Brander, K., *et al.*
751 (2007). Ecology: managing evolving fish stocks. *Science*, 318, 1247–1248.

752 Kwiatkowski, L., Torres, O., Bopp, L., Aumont, O., Chamberlain, M., Christian, J.R., *et al.*
753 (2020). Twenty-first century ocean warming, acidification, deoxygenation, and upper-
754 ocean nutrient and primary production decline from CMIP6 model projections.
755 *Biogeosciences*, 17, 3439–3470.

756 Lefort, S., Aumont, O., Bopp, L., Arsouze, T., Gehlen, M. & Maury, O. (2015). Spatial and
757 body-size dependent response of marine pelagic communities to projected global
758 climate change. *Global Change Biology*, 21, 154–164.

759 Lindmark, M., Ohlberger, J. & Gårdmark, A. (2022). Optimum growth temperature declines
760 with body size within fish species. *Global Change Biology*, 28, 2259–2271.

761 Lorenzen, K. (2016). Toward a new paradigm for growth modeling in fisheries stock
762 assessments: Embracing plasticity and its consequences. *Fisheries Research*, Growth:
763 theory, estimation, and application in fishery stock assessment models, 180, 4–22.

764 Lotze, H.K., Tittensor, D.P., Bryndum-Buchholz, A., Eddy, T.D., Cheung, W.W.L.,
765 Galbraith, E.D., *et al.* (2019). Global ensemble projections reveal trophic
766 amplification of ocean biomass declines with climate change. *Proceedings of the
767 National Academy of Sciences*, 116, 12907–12912.

768 Mackenzie, B.R., Gislason, H., Möllmann, C. & Köster, F.W. (2007). Impact of 21st century
769 climate change on the Baltic Sea fish community and fisheries. *Global Change
770 Biology*, 13, 1348–1367.

771 McCauley, D.J., Pinsky, M.L., Palumbi, S.R., Estes, J.A., Joyce, F.H. & Warner, R.R.
772 (2015). Marine defaunation: Animal loss in the global ocean. *Science*, 347.

773 McCoy, M.W. & Gillooly, J.F. (2008). Predicting natural mortality rates of plants and
774 animals. *Ecology Letters*, 11, 710–716.

775 Mion, M., Haase, S., Hemmer-Hansen, J., Hilvarsson, A., Hüssy, K., Krüger-Johnsen, M., *et
776 al.* (2021). Multidecadal changes in fish growth rates estimated from tagging data: A
777 case study from the Eastern Baltic cod (*Gadus morhua*, Gadidae). *Fish and Fisheries*,
778 22, 413–427.

779 Mion, M., Thorsen, A., Vitale, F., Dierking, J., Herrmann, J.P., Huwer, B., *et al.* (2018).
780 Effect of fish length and nutritional condition on the fecundity of distressed Atlantic
781 cod *Gadus morhua* from the Baltic Sea: POTENTIAL FECUNDITY OF BALTIC G.
782 *MORHUA*. *Journal of Fish Biology*, 92, 1016–1034.

783 Möllmann, C., Diekmann, R., Müller-Karulis, B., Kornilovs, G., Plikshs, M. & Axe, P.
784 (2009). Reorganization of a large marine ecosystem due to atmospheric and
785 anthropogenic pressure: a discontinuous regime shift in the Central Baltic Sea. *Global
786 Change Biology*, 15, 1377–1393.

787 Morán, X.A.G., López-Urrutia, Á., Calvo-Díaz, A. & Li, W.K.W. (2010). Increasing
788 importance of small phytoplankton in a warmer ocean. *Global Change Biology*, 16,
789 1137–1144.

790 Morita, K., Fukuwaka, M., Tanimata, N. & Yamamura, O. (2010). Size-dependent thermal
791 preferences in a pelagic fish. *Oikos*, 119, 1265–1272.

792 Munch, S.B. & Salinas, S. (2009). Latitudinal variation in lifespan within species is explained
793 by the metabolic theory of ecology. *Proceedings of the National Academy of Sciences*,
794 106, 13860–13864.

795 Neubauer, P. & Andersen, K.H. (2019). Thermal performance of fish is explained by an
796 interplay between physiology, behaviour and ecology. *Conserv Physiol*, 7.

797 Neuenfeldt, S., Bartolino, V., Orio, A., Andersen, K.H., Andersen, N.G., Niiranen, S., *et al.*
798 (2020). Feeding and growth of Atlantic cod (*Gadus morhua* L.) in the eastern Baltic
799 Sea under environmental change. *ICES Journal of Marine Science*, 77, 624–632.

800 Neuheimer, A.B. & Grønkjaer, P. (2012). Climate effects on size-at-age: growth in warming
801 waters compensates for earlier maturity in an exploited marine fish. *Global Change
802 Biology*, 18, 1812–1822.

803 Neuheimer, A.B., Thresher, R.E., Lyle, J.M. & Semmens, J.M. (2011). Tolerance limit for
804 fish growth exceeded by warming waters. *Nature Climate Change*, 1, 110–113.

805 Ohlberger, J. (2013). Climate warming and ectotherm body size – from individual physiology
806 to community ecology. *Functional Ecology*, 27, 991–1001.

807 Ohlberger, J., Edeline, E., Vollestad, L.A., Stenseth, N.C. & Claessen, D. (2011).
808 Temperature-driven regime shifts in the dynamics of size-structured populations. *The
809 American Naturalist*, 177, 211–223.

810 Pauly, D. (1980). On the interrelationships between natural mortality, growth parameters, and
811 mean environmental temperature in 175 fish stocks. *ICES Journal of Marine Science*,
812 39, 175–192.

813 Pinsky, M.L., Worm, B., Fogarty, M.J., Sarmiento, J.L. & Levin, S.A. (2013). Marine Taxa
814 Track Local Climate Velocities. *Science*, 341, 1239–1242.

815 Pontavice, H. du, Gascuel, D., Reygondeau, G., Maureaud, A. & Cheung, W.W.L. (2019).
816 Climate change undermines the global functioning of marine food webs. *Global
817 Change Biology*.

818 R Core Team. (2020). *R: A Language and Environment for Statistical Computing. R
819 Foundation for Statistical Computing*. Vienna, Austria.

820 Rall, B.C., Brose, U., Hartvig, M., Kalinkat, G., Schwarzmüller, F., Vucic-Pestic, O., *et al.*
821 (2012). Universal temperature and body-mass scaling of feeding rates. *Philosophical
822 Transactions of the Royal Society of London, Series B: Biological Sciences*, 367,
823 2923–2934.

824 Reum, J.C.P., Blanchard, J.L., Holsman, K.K., Aydin, K. & Punt, A.E. (2019). Species-
825 specific ontogenetic diet shifts attenuate trophic cascades and lengthen food chains in
826 exploited ecosystems. *Oikos*, 128, 1051–1064.

827 Righton, D.A., Andersen, K.H., Neat, F., Thorsteinsson, V., Steingrund, P., Svedäng, H.,
828 *et al.* (2010). Thermal niche of Atlantic cod *Gadus morhua*: limits, tolerance and
829 optima. *Marine Ecology Progress Series*, 420, 1–13.

830 van Rijn, I., Buba, Y., DeLong, J., Kiflawi, M. & Belmaker, J. (2017). Large but uneven
831 reduction in fish size across species in relation to changing sea temperatures. *Global
832 Change Biology*, 23, 3667–3674.

833 Rohatgi, A. (2012). *WebPlotDigitalizer: HTML5 based online tool to extract numerical data*
834 *from plot images. Version 4.1. [WWW document] URL*
835 *<https://automeris.io/WebPlotDigitizer> (accessed on January 2019).*

836 Savage, V.M., Gillooly, J.F., Brown, J.H., West, G.B. & Charnov, E.L. (2004). Effects of
837 body size and temperature on population growth. *The American Naturalist*, 163, 429–
838 441.

839 Scott, F., Blanchard, J. & Andersen, K. (2019). *mizer: Multi-Species sIZE Spectrum*
840 *Modelling in R*. R .

841 Scott, F., Blanchard, J.L. & Andersen, K.H. (2014). mizer: An R package for multispecies,
842 trait-based and community size spectrum ecological modelling. *Methods in Ecology*
843 *and Evolution*, 5, 1121–1125.

844 Scott, F., Blanchard, J.L. & Andersen, K.H. (2018). Multispecies, trait and community
845 size spectrum ecological modelling in R (mizer), 1–87.

846 Sheridan, J.A. & Bickford, D. (2011). Shrinking body size as an ecological response to
847 climate change. *Nature Climate Change*, 1, 401–406.

848 Steinacher, M., Joos, F., Frolicher, T.L., Bopp, L., Cadule, P., Cocco, V., *et al.* (2010).
849 Projected 21st century decrease in marine productivity: a multi-model analysis.
850 *Biogeosciences*, 7.

851 Svedäng, H. & Hornborg, S. (2014). Selective fishing induces density-dependent growth.
852 *Nature Communications*, 5, 4152.

853 Szwulski, C.S., Burgess, M.G., Costello, C. & Gaines, S.D. (2017). High fishery catches
854 through trophic cascades in China. *Proceedings of the National Academy of Sciences*,
855 114, 717–721.

856 Thorson, J.T., Monnahan, C.C. & Cope, J.M. (2015). The potential impact of time-variation
857 in vital rates on fisheries management targets for marine fishes. *Fisheries Research*,
858 169, 8–17.

859 Thorson, J.T., Munch, S.B., Cope, J.M. & Gao, J. (2017). Predicting life history parameters
860 for all fishes worldwide. *Ecological Applications*, 27, 2262–2276.

861 Thresher, R.E., Koslow, J.A., Morison, A.K. & Smith, D.C. (2007). Depth-mediated reversal
862 of the effects of climate change on long-term growth rates of exploited marine fish.
863 *Proceedings of the National Academy of Sciences, USA*, 104, 7461–7465.

864 Tittensor, D.P., Novaglio, C., Harrison, C.S., Heneghan, R.F., Barrier, N., Bianchi, D., *et al.*
865 (2021). Next-generation ensemble projections reveal higher climate risks for marine
866 ecosystems. *Nat. Clim. Chang.*, 11, 973–981.

867 Tu, C.-Y., Chen, K.-T. & Hsieh, C. (2018). Fishing and temperature effects on the size
868 structure of exploited fish stocks. *Sci Rep*, 8, 7132.

869 Ursin, E. (1967). A Mathematical Model of Some Aspects of Fish Growth, Respiration, and
870 Mortality. *Journal of the Fisheries Research Board of Canada*, 24, 2355–2453.

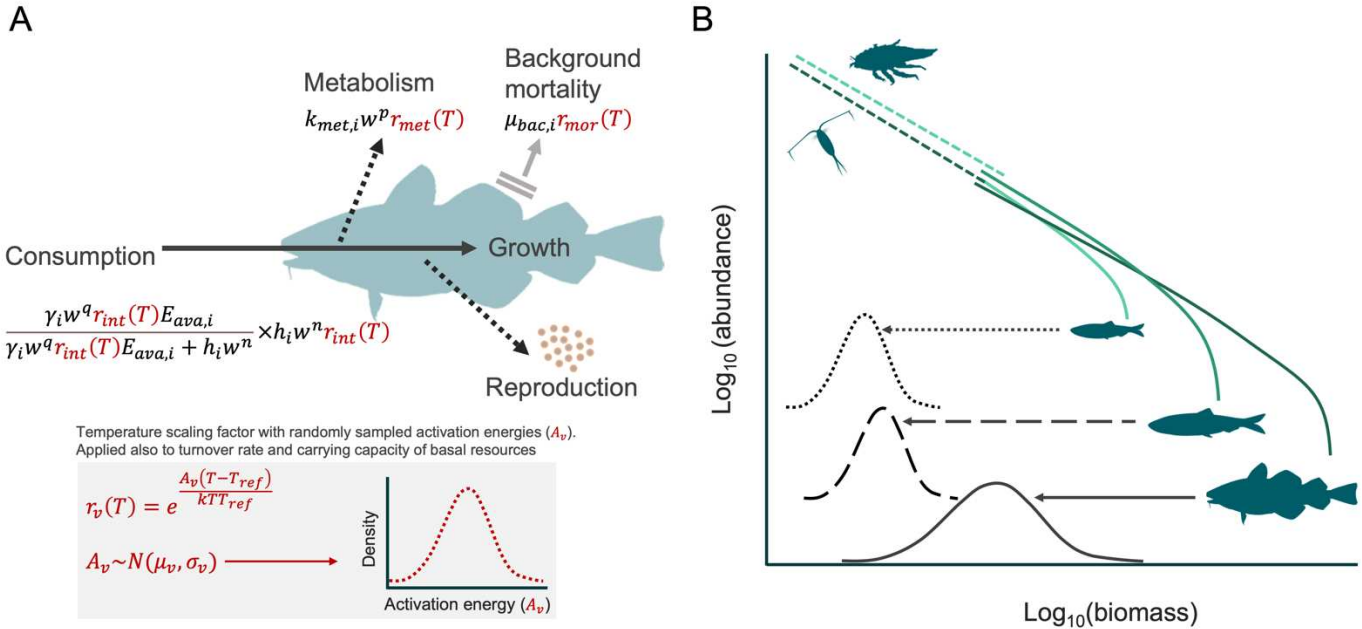
871 Ursin, E. (1973). On the prey size preferences of cod and dab. *Meddelelser fra Danmarks*
872 *Fiskeri-og Havun- dersgelser*, 7:8598.

873 Woodworth-Jefcoats, P.A., Blanchard, J.L. & Drazen, J.C. (2019). Relative Impacts of
874 Simultaneous Stressors on a Pelagic Marine Ecosystem. *Frontiers in Marine Science*,
875 6.

876 Woodworth-Jefcoats, P.A., Polovina, J.J., Dunne, J.P. & Blanchard, J.L. (2013). Ecosystem
877 size structure response to 21st century climate projection: large fish abundance
878 decreases in the central North Pacific and increases in the California Current. *Global*
879 *Change Biology*, 19, 724–733.

880 Woodworth-Jefcoats, P.A., Polovina, J.J., Howell, E.A. & Blanchard, J.L. (2015). Two takes
881 on the ecosystem impacts of climate change and fishing: Comparing a size-based and

882 a species-based ecosystem model in the central North Pacific. *Progress in*
883 *Oceanography*, 138, 533–545.
884 Yvon-Durocher, G., Montoya, J.M., Trimmer, M. & Woodward, G. (2011). Warming alters
885 the size spectrum and shifts the distribution of biomass in freshwater ecosystems.
886 *Global Change Biology*, 17, 1681–1694.
887
888
889
890
891
892
893
894
895
896
897
898
899
900
901
902



903

904 *Figure 1. (A) Schematic representation of the individual level energy fluxes and their temperature*
 905 *dependence, and (B) the abundance spectrum of fishes (solid lines) emerging from food-dependent*
 906 *growth and mortality, and spectra of their background pelagic and benthic resource (dashed lines).*

907

908

909

910

911

912

913

914

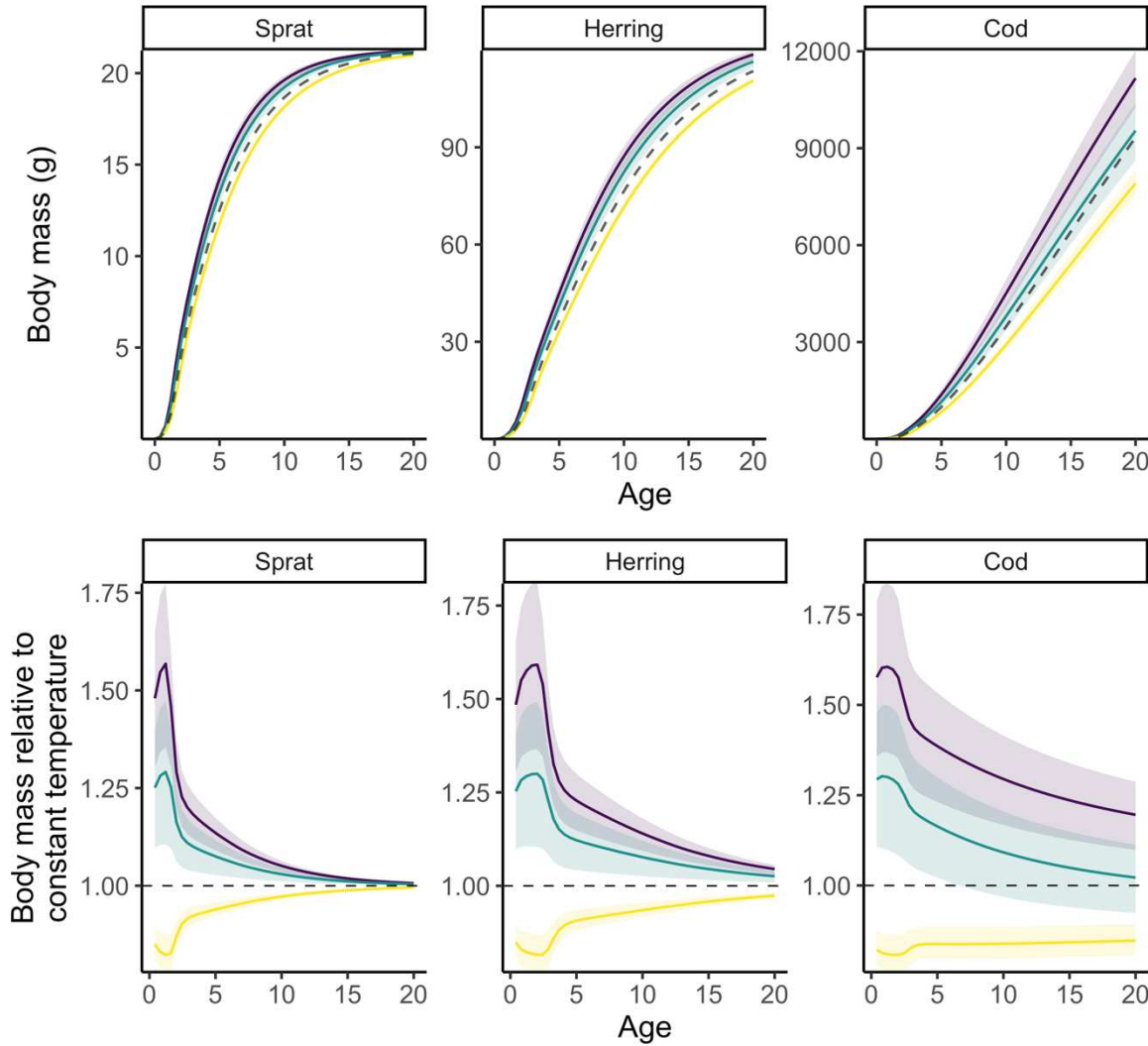
915

916

917

918

919



920

Scenario — Physio. — Physio. + Resource — Resource

921

Figure 2. Individual growth trajectories of sprat, herring, and cod from model projections to year 2050

922

assuming warming according to RCP 8.5 while keeping fishing mortality at F_{MSY} levels from the size

923

spectrum model. The dashed line in the top row depicts projections assuming a non-warming scenario

924

and thus constitutes a baseline prediction. Colours indicate different temperature-scaling scenarios.

925

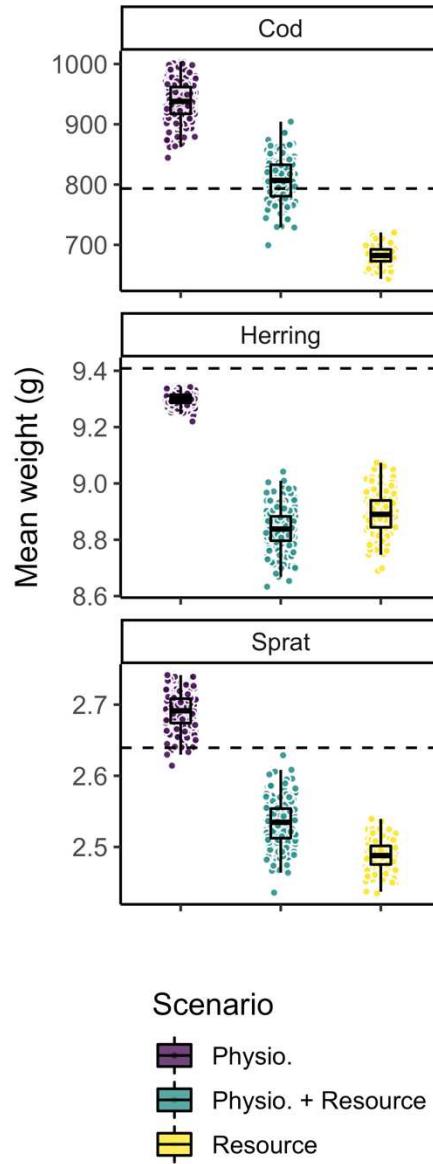
Shaded areas encompass the 2.5 and 97.5 percentiles from the set of 200 simulations with randomly

926

assigned activation energies.

927

928



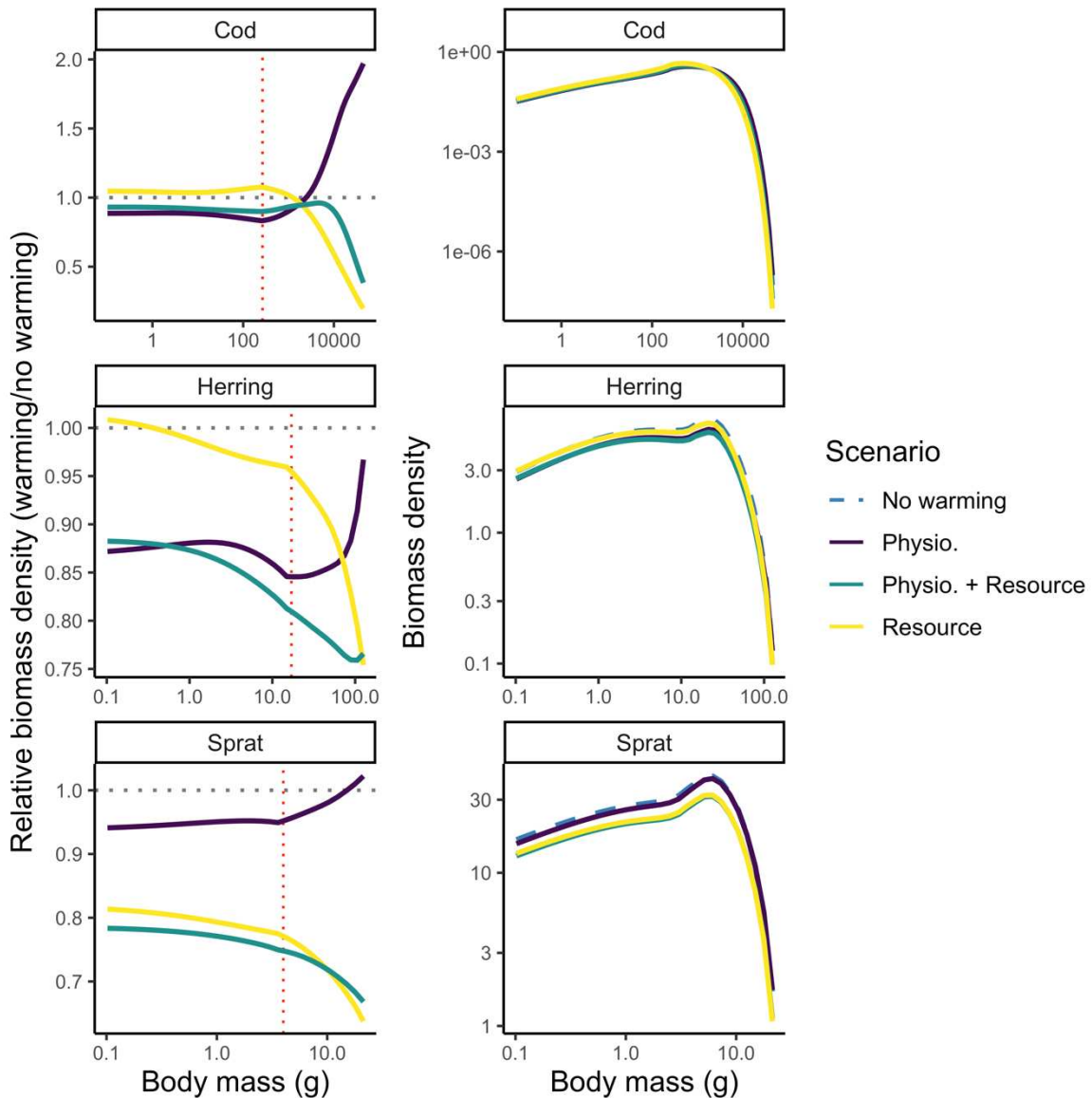
929

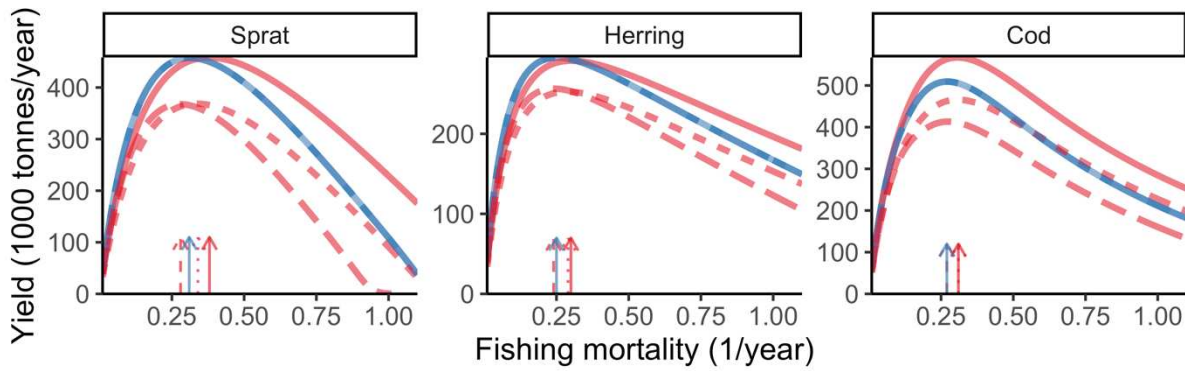
930 *Figure 3. Mean weight across all individuals in the populations of sprat, herring and cod from model*
931 *projections to year 2050 assuming warming according to RCP 8.5 while keeping fishing mortality at*
932 *F_{MSY} levels from the size spectrum model. The dashed horizontal line depicts projections assuming no*
933 *temperature increase and thus constitutes a baseline prediction. Each dot represents one of the 200*
934 *simulations, each with randomly assigned activation energies. Boxplots depict 25%, 50% and 75%*
935 *quantiles of the 200 simulations in each scenario.*

936

937

938





948 Temp. — T_{ref} — $T_{ref} + 2^\circ\text{C}$ Scenario — Physio. — Physio. + Resource — Resource

949 *Figure 5. Steady state biomass yield assuming knife edge selectivity at maturation size under two*
950 *constant temperature simulations and three scenarios for temperature dependence. Colours indicate*
951 *temperature, where blue means $T = T_{ref}$ (i.e., no temperature effects), and red depicts warm*
952 *temperature, here $T = T_{ref} + 2^\circ\text{C}$. Dashed lines correspond to resource dynamics being temperature*
953 *dependent, dotted lines correspond to physiological rates and resource dynamics being temperature*
954 *dependent and solid lines depicts only physiological temperature scaling. Arrows indicate fishing*
955 *mortality (F) that leads to maximum sustainable yield (F_{MSY}). F is held constant at the mean F during*
956 *calibration (mean 1992-2002) for the two other species while estimating yield curves for one species.*
957 *Note the different scales between species. Only mean activation energies are used (Table S3, Supporting*
958 *Information).*

959

960

961

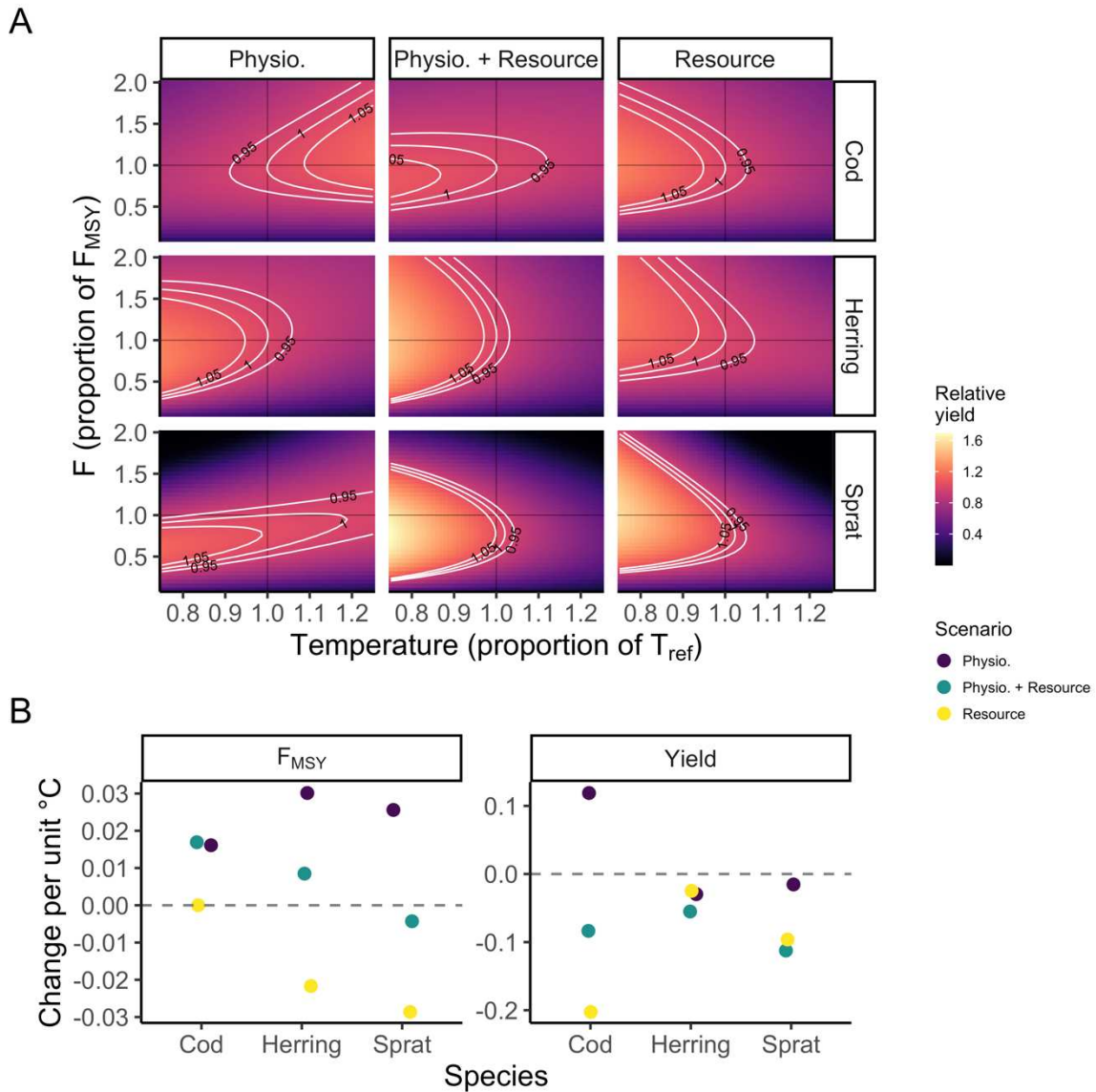
962

963

964

965

966



967

968 *Figure 6. Example of fisheries yield (A) at steady state relative to MSY at T_{ref} (no effect of temperature)*
 969 *from simulations with constant (not time-varying) temperatures with the three temperature dependence*
 970 *scenarios (columns), and how F_{MSY} and yields change with temperature. In panel A, The y-axis shows*
 971 *fishing mortality, F , as a proportion to F_{MSY} (as estimated from the size spectrum model) at T_{ref} and*
 972 *the x-axis shows temperature as a proportion of T_{ref} . The other two species are held at their F_{MSY} when*
 973 *one species' F is varied. Panel B shows slopes of F_{MSY} (left) and yield (right) over temperature. Only*
 974 *mean activation energies are used (Table S3, Supporting Information).*